



**HAL**  
open science

## Modeling and CFD Study of Heat Transfer within the Circulation Pipes of Solar Water Heating Systems

T. Bouhal, Y. Agrouaz, Tarik Kousksou, A. Jamil, Youssef Zeraouli, A. Elouali, T. El Rhafiki, M. Bakkas

### ► To cite this version:

T. Bouhal, Y. Agrouaz, Tarik Kousksou, A. Jamil, Youssef Zeraouli, et al.. Modeling and CFD Study of Heat Transfer within the Circulation Pipes of Solar Water Heating Systems. International Renewable and Sustainable Energy Conference, IRSEC 2016, Nov 2016, Marrakech, Morocco, Morocco. pp.258-263, <10.1109/IRSEC.2016.7983919>. <hal-02154004>

**HAL Id: hal-02154004**

**<https://univ-pau.hal.science/hal-02154004v1>**

Submitted on 8 Oct 2020

HAL is a multi-disciplinary open access archive for the deposit and dissemination of scientific research documents, whether they are published or not. The documents may come from teaching and research institutions in France or abroad, or from public or private research centers.

L'archive ouverte pluridisciplinaire HAL, est destinée au dépôt et à la diffusion de documents scientifiques de niveau recherche, publiés ou non, émanant des établissements d'enseignement et de recherche français ou étrangers, des laboratoires publics ou privés.



Distributed under a Creative Commons CC BY 4.0 - Attribution - International License

# Modeling and CFD Study of Heat Transfer Within the Circulation Pipes of Solar Water Heating Systems

Tarik Bouhal<sup>a,b,\*</sup>, Younes Agrouaz<sup>a,b</sup>, Tarik Kousksou<sup>b</sup>,  
Abdelmajid Jamil<sup>a</sup>, Youssef Zeraoui<sup>b</sup>

<sup>a</sup> Université Sidi Mohamed Ibn Abdelah  
Ecole Supérieure de Technologie EST  
Fès, Morocco

<sup>b</sup> Laboratoire des Sciences de l'Ingénieur Appliquées à la  
Mécanique et au Génie Electrique (SIAME), UPPA  
Pau, France

Abdelmajid Elouali, Tarik El Rhafiki, M'bark Bakkas  
Université Moulay Ismail  
Ecole Nationale Supérieure d'Arts et Métiers ENSAM  
Meknès, Morocco  
bouhal.tarik12@gmail.com

\*

**Abstract**— The main objective of this work is to study numerically the thermal behavior of solar collectors. In particular, we performed a detailed design and parametric study of the circulation pipe of an evacuated tube collector. Indeed, we altered the geometry of the anodes by adopting three configurations: circular, rectangular and triangular. In each configuration, we changed the inlet position of cold water and the outlet of hot water: either at the top, middle or bottom. The obtained results show that rectangular shape is most optimal due to the large exchange area. On the other hand, the water inlet must be positioned at the bottom and the outlet at the top in order to take profit of the stratification of the hot water and subsequently obtain high efficiency.

**Keywords:** Solar Water Heating Systems; Anodes, Heat Flux, CFD.

## I. INTRODUCTION

Actually, intensive efforts have been made in attempt to either integrate or replace conventional energy sources with renewable energy sources (RES) in order to meet power demands [1]. This is due to the fact that RES are non-polluting and non-depletable whilst they also have low operation and maintenance costs thus making them potential sources of alternative energy [1-2]. Solar water heating systems (SWHS) are among the most common and favorable renewable energy systems as the use of these systems can result in significant energy savings. However, there are limiting factors to be considered when utilizing SWHS. These include: unpredictable behavior (energy produced from renewable energy sources may not always meet the demand), economic viability and thermal performance.

It is important to investigate ways to overcome these limitations so as to increase the viability of SWHS. A common solution to these problems is the use of an effective thermal energy storage system (one that is able to store thermal energy at the highest possible temperature whilst exhibiting minimal thermal losses). The main thermal energy storage techniques include: thermally stratified storage and reversible chemical heat storage [3]. A second method, conducted in the present study, involves to an optimization study on the design of equipment sentatives significant energy loss as the storage tank, the pipes of circuits circulation in order to increase the

rate of energy transfer thereby maximizing energy transfer from the solar collector to the energy storage units (tanks).

This paper focuses on thermal behaviour of solar collectors and aims to provide some information on thermal performance of the circulation pipe of an evacuated tube collector. So, the layout of this paper is as follows: The problem formulation and schematic configuration are presented in Section 2. The formulation of the physical model is presented in Section 3. In Section 5, a parametric study is presented together with a discussion and analysis of the corresponding results.

## Nomenclature

$g$	[ $\text{ms}^{-2}$ ]	Gravitational acceleration
$R_a$	[-]	Rayleigh number
$N_u$	[-]	Average Nusselt number
$P_r$	[-]	Prandtl number
$C_p$	[ $\text{Jkg}^{-1}\text{K}^{-1}$ ]	Heat capacity
$T_m$	[K]	Reference temperature

## Special characters

$\alpha$	[ $\text{m}^2\text{s}^{-1}$ ]	Effective thermal diffusivity
$\beta$	[ $\text{K}^{-1}$ ]	Coefficient of thermal expansion
$\nu$	[ $\text{m}^2\text{s}^{-1}$ ]	Kinematic viscosity
$\rho$	[ $\text{kgm}^{-3}$ ]	Fluid density

## II. DEFINITIONS OF SCHEMATIC CONFIGURATIONS

In current paper, we are interested in an alternative of evacuated solar collectors where the storage tank is separated from the vacuum tube as represented in Figure 1.



Figure 1. Circulation pipe of evacuated tube collector

The geometry adopted is a straight pipe. The physical model considered is shown schematically in Figure 2. We imposed a temperature of  $90^\circ\text{C}$  at the anodes, the rest is maintained adiabatic except the inlet and outlet pipe in which we have imposed an inlet speed water of  $1 \text{ m}\cdot\text{s}^{-1}$ . The initial temperature of the inlet water is equal to  $15^\circ\text{C}$ .

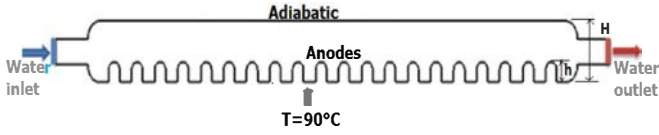


Figure 2. Representative domains used for thermal modelling

In this paper, we studied different geometries of the anodes and different positions of inlet and outlet water. The ratio  $\frac{h}{H} = 0.2$  is maintained constant for all configurations. Moreover, the water enters to pipe with a speed of and exits after it is heated by the temperature imposed on the anodes. In the current investigation, we studied different configurations as shown in Figures 3, 4 and 5. On this way, we altered the geometry of the anodes by adopting three configurations: circular, rectangular and triangular. In each configuration, we changed the inlet position of cold water and the outlet of hot water: either at the top, middle or bottom.

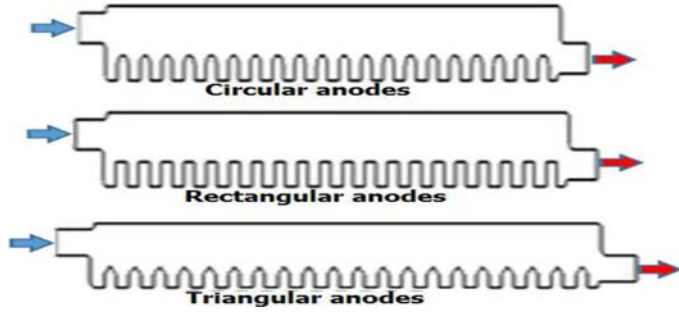


Figure 3. Schematic of pipe with three anodes shape: Circular, Rectangular and Triangular, Inlet in top and outlet in bottom

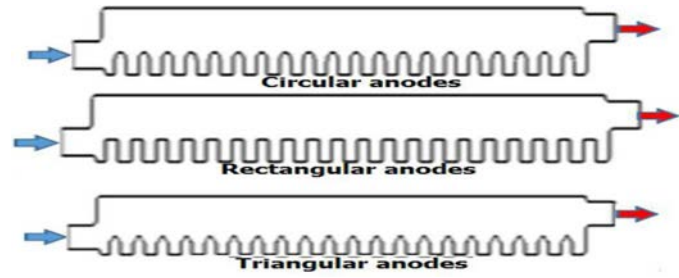


Figure 4. Schematic of pipe with three anodes shape: Circular, Rectangular and Triangular, Inlet in bottom and outlet in top

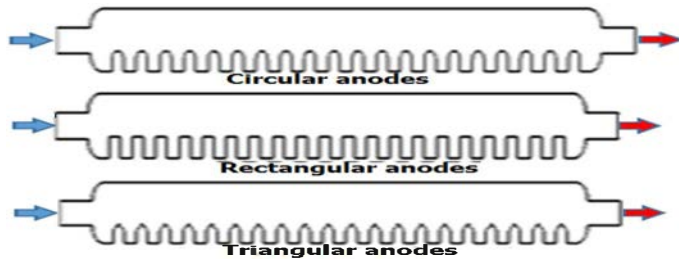


Figure 5. Schematic of pipe with three anodes shape: Circular, Rectangular and Triangular, Inlet and outlet in the middle

### III. PHYSICAL MODEL AND BASIC EQUATIONS

The following assumptions are made in the analysis:

- The Boussinesq approximation is valid, i.e., liquid density variations arise only in the buoyancy source term, but are otherwise neglected.
- The water is Newtonian.
- Viscous dissipation is neglected.
- Fluid motion is laminar and two-dimensional.

With the foregoing assumptions, the conservation equations for mass, momentum and energy may be stated as:

$$\int_S \vec{u} \cdot \vec{n} dS = 0 \quad (1)$$

$$\frac{d}{dt} \int_V \rho \vec{u} dV + \int_S \rho \vec{u} \vec{u} \cdot \vec{n} dS = - \int_V \vec{\nabla} p dV + \int_S \vec{\tau} \cdot \vec{n} dS + \int_V \vec{A}_U dV \quad (2)$$

$$\frac{d}{dt} \int_V \rho c_p T dV + \int_S \rho c_p T \vec{u} \cdot \vec{n} dS = \int_S \lambda \vec{\nabla} T \cdot \vec{n} dS \quad (3)$$

Where  $\vec{u}$  is the velocity vector,  $p$  the pressure and  $T$  the temperature and  $\vec{\tau}$  is the viscous stress tensor for a Newtonian fluid:

$$\vec{\tau} = \mu \left( \vec{\nabla} \vec{u} + (\vec{\nabla} \vec{u})^T \right) \quad (4)$$

The integration occurs over a control volume  $V$  surrounded by a surface  $S$ , which is oriented by an outward unit normal vector  $\vec{n}$ . The source term in Eq.(2) contains two parts:

$$\vec{A}_U = \rho \beta (T - T_m) \vec{g} \quad (5)$$

Where  $\beta$  is the coefficient of volumetric thermal expansion and  $\vec{g}$  the acceleration of gravity vector. The first part of the term source represents the buoyancy forces due to the thermal dilatation. In Eq.(5),  $T_m$  is the reference temperature.

The conservation Eqs.1-3 are solved by implementing them in a house code. This code has been successfully validated in several situations involving flow and heat transfer as in [4-5].

### IV. RESULTS AND DISCUSSION

In the current paper, we developed a parametric study on three types of anodes by changing their geometry: rectangular, circular and triangular anodes. The factors that we varied in the current study is the location of the pipe inlet and outlet. We will presented for each form the temperature field and the outlet temperature, the streamlines and the Nusselt number on the heated source. For all simulations performed in this study, we adopted approximately a Prandtl number equal to 7 (Which corresponds to water).

#### Thermal fields

Figures 6, 7 and 8 show the spatial and temporal distribution of the temperature field inside the pipe for various inlet/outlet positions and for different anodes configurations: circular, triangular and rectangular. The thermal field is represented by the contours of the temperatures. Border anodes, down the pipe, we find that the effect of conduction

transfer phenomenon is more dominant than convection. If we compare the isotherms in the all figures for different geometric shapes, it may be noted that when changing the geometry, the isothermal approach each other in the area near the lower wall heated i.e that the gradients of the temperature becomes higher near the bottom wall heated. This implies an increase in the heat transfer through the bottom wall of the pipe. So we can say that the higher temperatures are those of the fluid flowing in parallel with the heated wall, while the lower temperatures are those of the fluid which circulates parallel to the cold walls. Thus, the fluid is heated in contact with the heated region, cools in contact with the cold walls.

When changing the positions of water inlet and outlet, the heat recovered from the heat source is conveyed by forced convection to the top and near to pipe outlet by the heat anodes and water velocity. This is what explains the relatively high temperatures in the bottom portion of the pipe, the heat is dissipated fairly through both the water inlet and outlet.

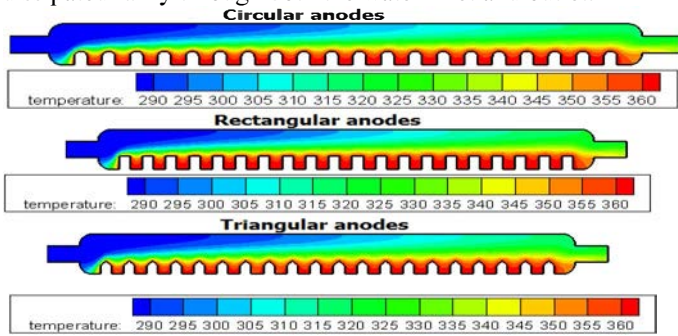


Figure 6. Isotherms inside the pipe for various geometrical anodes: Inlet and outlet in middle

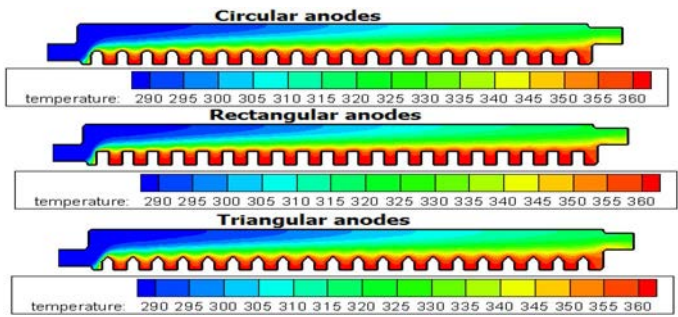


Figure 7. Isotherms inside the pipe for various geometrical anodes: Inlet in bottom and outlet in top

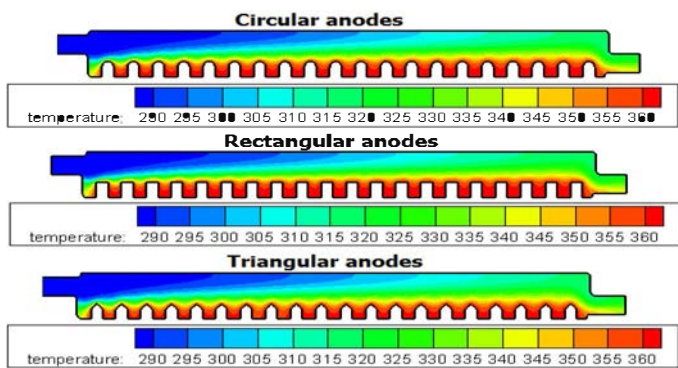


Figure 8. Isotherms inside the pipe for various geometrical anodes: Inlet in top and outlet in bottom

### Average and outlet temperatures evolution for various geometrical anodes: Inlet and outlet in middle

Figure 9 depict the average and outlet temperatures inside the pipe during 10 min of simulation for a circular anodes case. The water inlet and are both chosen in middle. From the graph it can be observed that the evolution of the output temperature is slow. Initially, the water comes out at 15°C and then its outlet temperature grow slowly until reaching 55 °C for 10 min.

Contrariwise, the water average temperature inside interior pipe increases rapidly due to anodes which are used to heat water to an average temperature of 45°C.

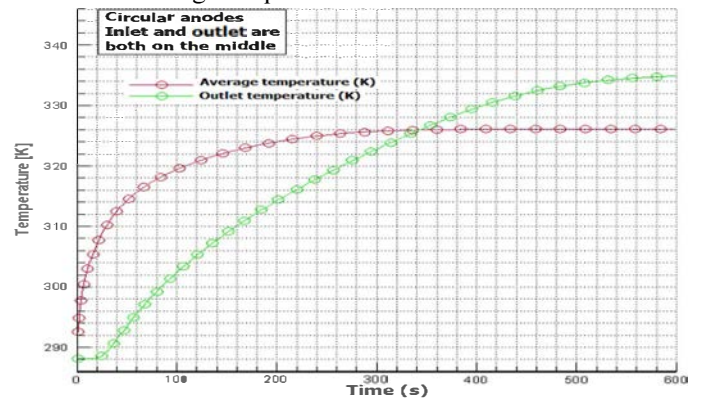


Figure 9. Average and outlet temperatures evolution for circular anodes case: Inlet and outlet in middle

Figure 10 shows the evolution of the water temperature at the outlet and the average temperature within the pipe for the case of a rectangular anodes geometry. The inlet/outlet are positioned in the middle of the pipe. After about 5min, the outlet temperature reaches 55°C while the average temperature does not exceed 45°C.

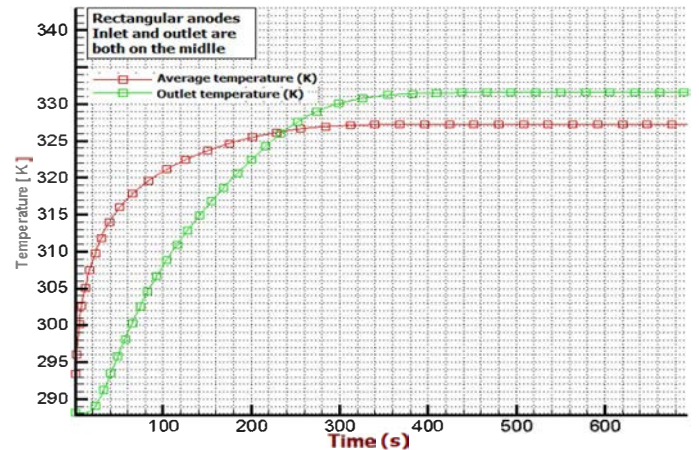


Figure 10. Average and outlet temperatures evolution for rectangular anodes case: Inlet and outlet in middle

For the case of a triangular anodes geometry, Figure 11 shows the evolution of the water temperature at the outlet and the average temperature within the pipe. The inlet/outlet are positioned in the middle of the pipe. After about 5min, the average temperature does not exceed 45°C while the outlet temperature reaches 55°C.

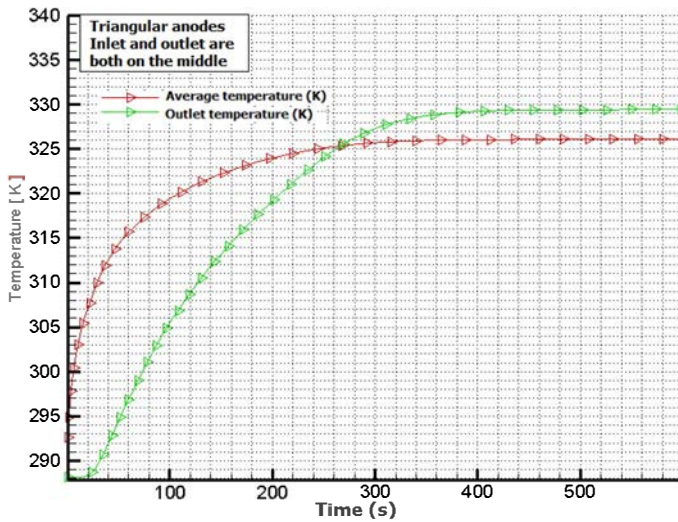


Figure 11. Average and outlet temperatures evolution for triangular anodes case: Inlet and outlet in middle

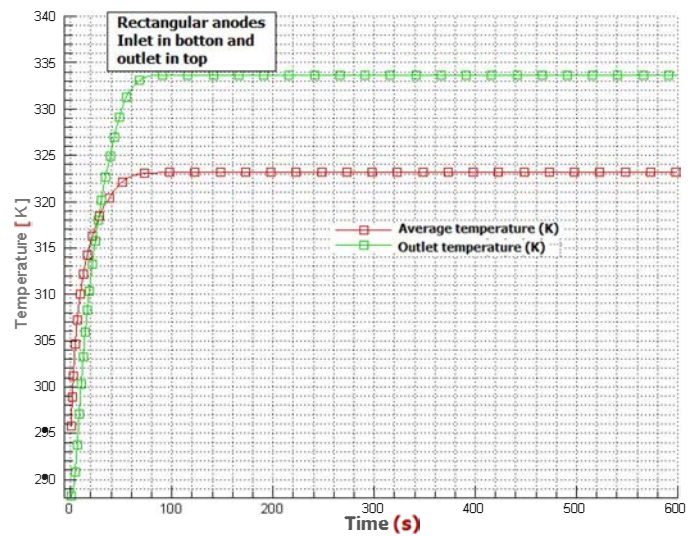


Figure 13. Average and outlet temperatures evolution for rectangular anodes case: Inlet in bottom and outlet in top

**Average and outlet temperatures evolution for various geometrical anodes: Inlet in bottom and outlet in top**

In this case, we changed the water inlet position in bottom while the outlet is positioned at the top of the pipe. The same trends can be noticed. Indeed, the outlet temperature exceeds 60°C for 5 min and the water average temperature is homogenized rapidly and reaches 45°C (see Figure 12).

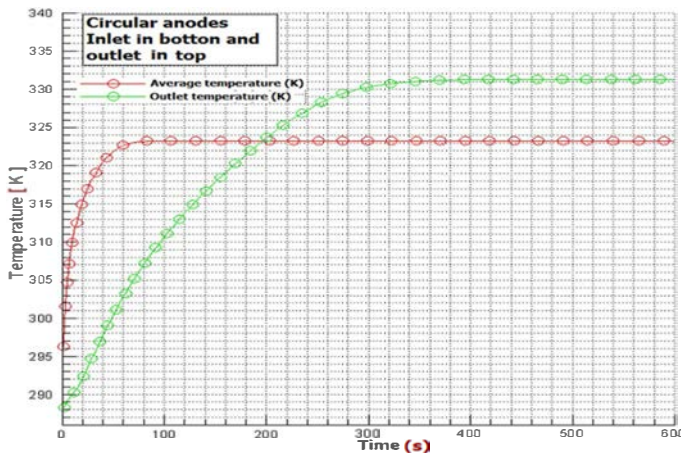


Figure 12. Average and outlet temperatures evolution for circular anodes case: Inlet in bottom and outlet in top

When the water inlet is positioned at the bottom and outlet at the top for a rectangular anodes, water heats up and increases rapidly to a temperature of 60°C while the average temperature does not exceed 45°C (see Figure 13).

For the triangular geometry of the anodes, the input and outputs are maintained down and up respectively. The outlet temperature reaches 60°C while the average temperature is changing rapidly inside the pipe and reaches 50°C.

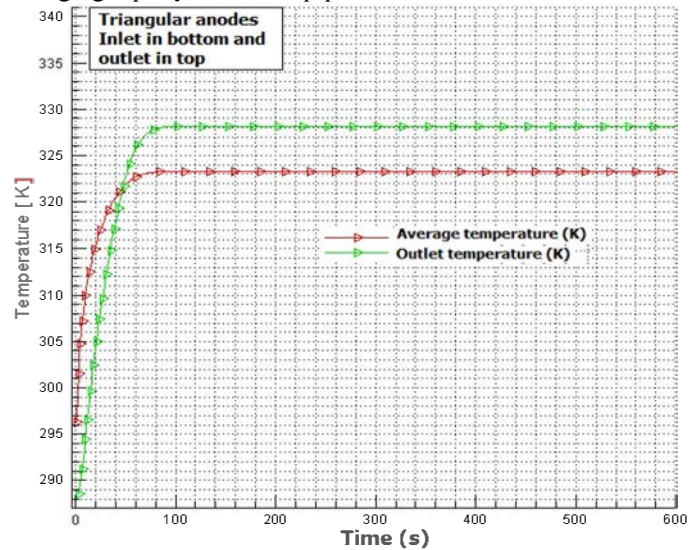


Figure 14. Average and outlet temperatures evolution for triangular anodes case: Inlet in bottom and outlet in top

**Average and outlet temperatures evolution for various geometrical anodes: Inlet in top outlet in bottom**

In Figure 15, when switching the input/output position with an input at the top and the outlet at the bottom for a circular geometry of anodes, the average temperature does not exceed 45°C but the outlet temperature reaches more than 60°C.

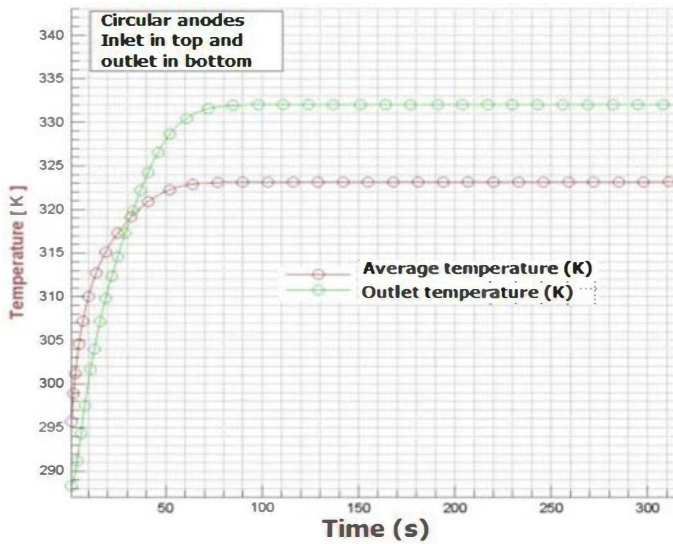


Figure 15. Average and outlet temperatures evolution for circular anodes case: Inlet in top and outlet in bottom

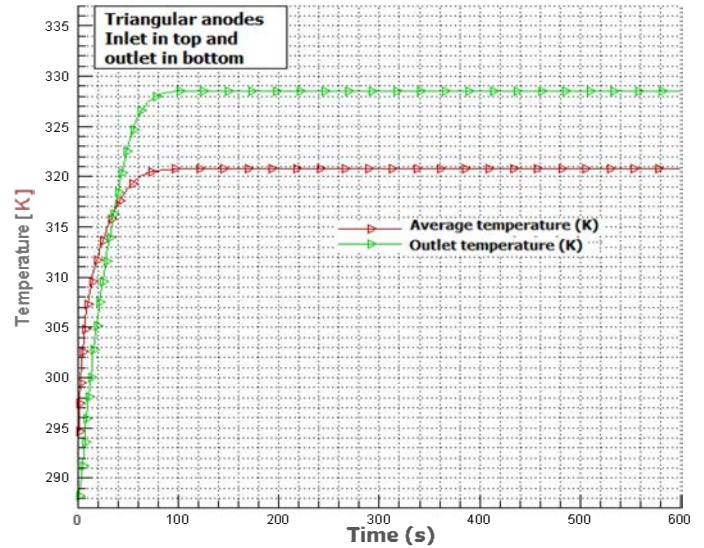


Figure 17. Average and outlet temperatures evolution for triangular anodes case: Inlet in top and outlet in bottom

In this case, almost the same trend can be noted. The output temperature exceeds  $60^{\circ}\text{C}$  in a quick time but the average temperature does not exceed  $45^{\circ}\text{C}$  (see Figure 16).

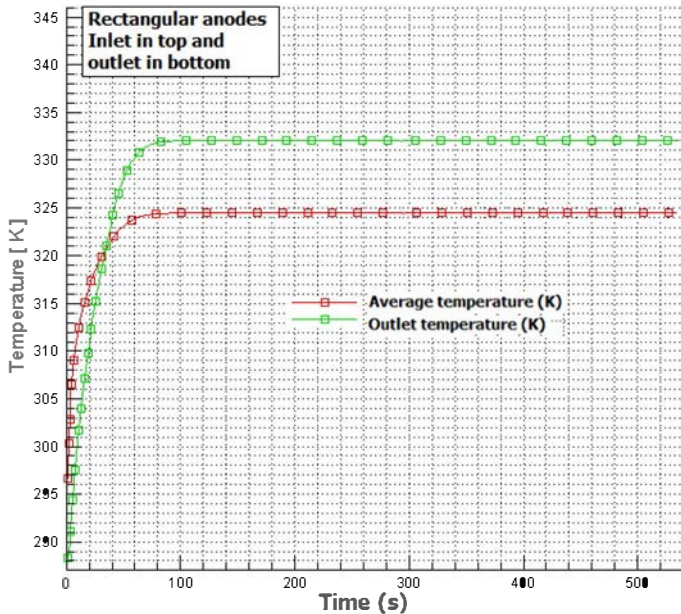


Figure 16. Average and outlet temperatures evolution for rectangular anodes case: Inlet in top and outlet in bottom

For triangular anodes, the water inlet at the top position and the bottom outlet, the outlet temperature exceeds  $60^{\circ}\text{C}$  and water of the interior pipe keeps a temperature of  $45^{\circ}\text{C}$ .

For all configurations studied previously and for various input /output positions, we notice that the evolution of average temperature in the middle and output is a function of time. After a few minutes the system is established and the temperature reaches about  $45^{\circ}\text{C}$ .

### Comparison between different geometrical anodes: Outlet temperature evolution for various inlet/outlet positions

To compare between different geometries of anodes and to assess the optimal location of the water input/output, we based on the water outlet temperature as a criterion. Indeed, the aim is to heat the water inside the pipe therefore the most appropriate form which delivers the highest output temperature in a minimum time.

The graphs referring to figures 18, 19 and 20 depict the output temperature evolution for all anode's geometry and various inlet/outlet positions. All obtained results show that the rectangular shape is most optimal given the large surface area.

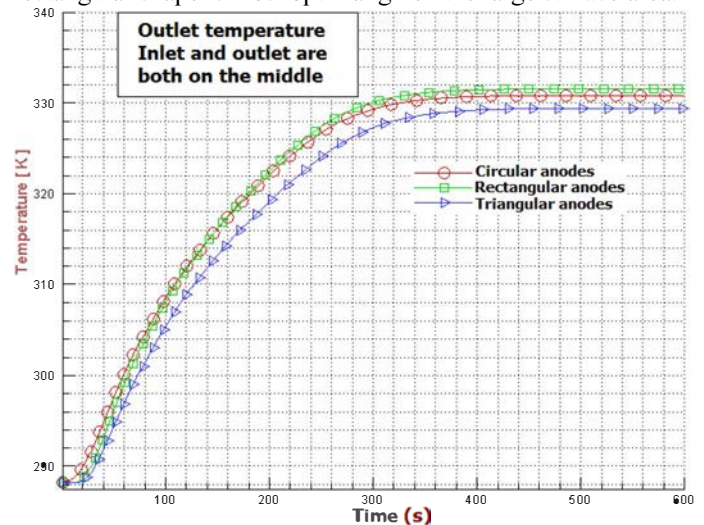


Figure 18. Outlet temperature evolution for various geometrical anodes: Inlet and outlet in middle

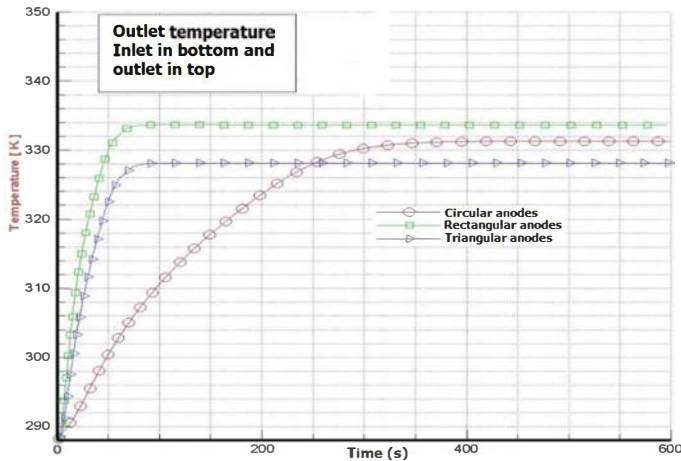


Figure 19. Outlet temperature evolution for various geometrical anodes: Inlet in bottom and outlet in top

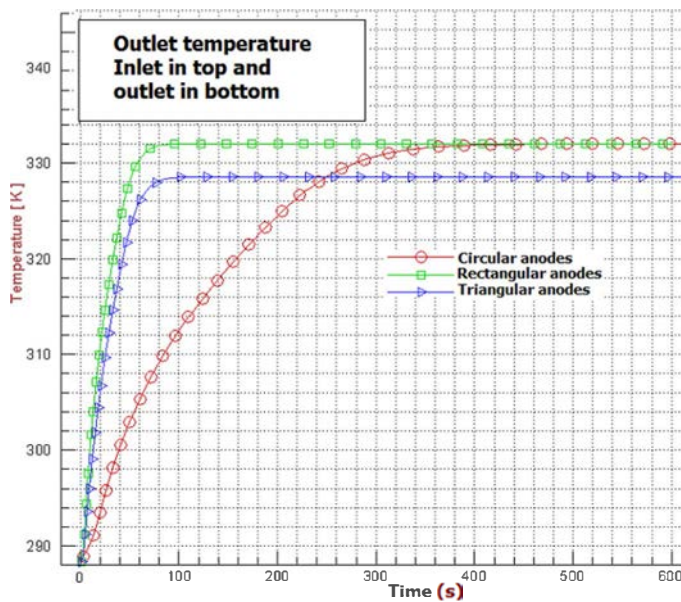


Figure 20. Outlet temperature evolution for various geometrical anodes: Inlet in top and outlet in bottom

### Comparison between inlet/outlet positions for rectangular anodes case

The results presented previously showed that the rectangular shape is the most optimal thanks to the large exchange surface. The objective is to select the optimal location of the water inlet/outlet based on the outlet temperature. Figure 21 shows the outlet temperature evolution for different positions. The figure demonstrates that the water inlet must be positioned at the bottom and outlet at the top to take advantage of the stratification of the hot water and thereafter obtain a maximum efficiency.

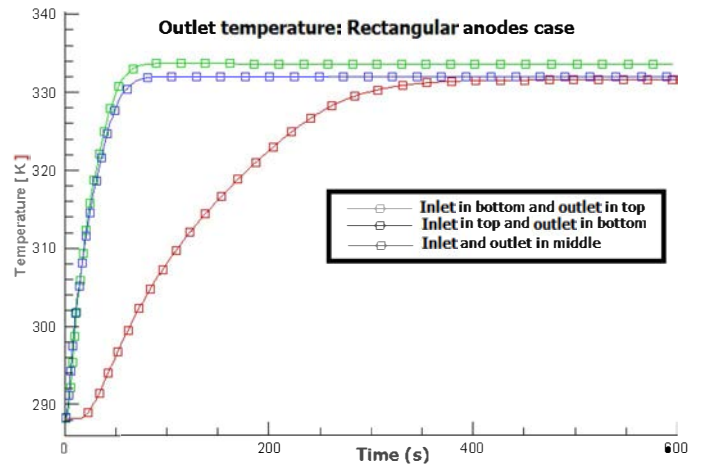


Figure 21. Outlet temperature evolution for various inlet/outlet positions: Rectangular anodes case

## V. CONCLUSION

In this study, we performed a numerical simulation on three anodes geometry types for a pipe used in an evacuated tube collector. The results obtained show, firstly that the rectangular shape is the most optimal thanks to the large surface area. On the other hand, the water inlet must be positioned at the bottom and outlet at the top to take advantage of the stratification of the hot water and subsequently obtain high performance.

## ACKNOWLEDGMENT

This work has been carried out within the project of Solar Cooling Process in Morocco (SCPM) thanks to the support of “Institut de Recherche en Energie Solaire et Energies Nouvelles IRESEN-Morocco”.

## REFERENCES

- [1] Y. Guo, M. Pan, Y. Fang, Optimal power management of residential customers in the smart grid, *Parallel Distrib. Syst. IEEE Trans.* 23 (9) (2012) 1593e1606.2002, pp. 25-34
- [2] M. Pedrasa, T. Spooner, I. MacGill, Coordinated scheduling of residential distributed energy resources to optimize smart home energy services, *Smart Grid IEEE Trans.* 1 (2) (2010) 134e143.
- [3] A. Barbato, A. Capone, G. Carello, M. Delfanti, M. Merlo, A. Zaminga, Cooperative and non-cooperative house energy optimization in a smart grid perspective, in: *World of Wireless, Mobile and Multimedia Networks (WoWMoM)*, 2011 IEEE International Symposium on a, 2011, pp. 1e6.
- [4] T. Kousksou, M. Mahdaoui, A. Ahmed, A. Ait Msaad, Melting over a wavy surface in a rectangular cavity heated from below, *Energy* 2013, In press.
- [5] A. Arid, T. Kousksou, S. Jegadheeswaran, A. Jamil, Y. Zeraoui, Numerical simulation of ice Melting near the density inversion point under periodic thermal boundary conditions, *Fluid Dynamics Materials Processing* 305 (2012) 1-19.